Experimental Evaluation of Divisible Human-Robot Shared Control for Teleoperation Assistance

Keng Peng Tee*, Yan Wu

***Abstract*— This paper is concerned with divisible shared control, which decomposes the motion space into complementary subspaces and distributes the control to the human and the robot so that each can independently effect motion control in its subspace. We present a divisible shared control scheme to assist teleoperation tasks on a curved object surface, which is difficult for a human to perform without assistance. We designed and carried an experiment to investigate its effect of user performance and work load. Experimental evaluation, based on both quantitative and qualitative measures, suggests that divisible shared control improves accuracy, speed, and smoothness, while at the same time reduces cognitive load, effort, and frustration.**

I. Introduction

The study of human-robot collaboration is useful as it helps to shed light on how to best combine the complementary proficiencies of human and robot to yield better performance and efficiency in practical applications such as teleoperation [1], [2], coassembly [3], automated driving [4], and rehabilitation [5].

The concept of divisible, interactive, and antagonistic tasks for human-robot or human-human interactions was discussed in [6]. Divisible tasks are tasks which are composed of subtasks that each agent can independently carry out. They include cases where the tasks are decomposed into regions, where each agent performs the part of the task related to its designated region, or in terms of time, where each agent perform its subtask in a sequential manner after the other agent has completed its subtask. More interestingly, divisible tasks also include those that can be split into disjunct but complementary subspaces, such the translation and rotational subspaces in rigid transformations. On the other hand, interactive and antagonistic tasks are those where there is no clear way of defining an independent subtask for each agent and/or when the actions of an agent significantly affects the performance of the other agent.

Based on this categorization of tasks in the context of multi-agent interactions, we similarly classify human-robot shared control into divisible and interactive categories, with focus on teleoperative applications. Divisible shared control distributes the control to the human and the robot in a way that each agent can independently control a subtask. Additionally, non-performance or bad performance of an agent in its subtask does not affect the performance of the other agent in performing its subtask, although the overall task may not be completed. Erden and Maric [7] studied manual welding, assisted by a robot, which complemented the human's dexterous control with its own vibration filtering and speed measurement, thereby improving the performance of novice welders. Sreekanth et al [8] looked into curve-following tasks where the human kinesthetically guides the speed with which a robot moves along a predefined 3D path, aided by impedance control to restore the effector towards the path in the presence of lateral deviations. Such approaches of constraining motion along certain paths while preventing excursions into other forbidden zones are also called virtual fixture methods, and were investigated previously for surgical assistance robots and for aiding telemanipulation [9]-[11].

For interactive shared control, each agent's control subspace overlaps with that of the other agent, and so there is a direct effect of the other agent's task performance, and vice versa, that needs to be resolved. Each agent has to attempt to either reject the other agent's effect, comply with it, or achieve a middle ground between the two. A continuous human-robot role adaptation method was proposed in [12] which adapts the robot's control gain under a game-theoretic framework based on kinesthetic disagreements from the human. This adaptive method was improved in [13] by using neural network based policy iteration to obviate the need for an explicit model of the human dynamics. Other approaches include risk-sensitive optimal control to adaptively switch between model-based and model-free predictions [14] and homotopy-based switching control to dynamically change the roles between leader and follower [15].

In this paper, we focus on divisible shared control, and investigate its use in assisting teleoperation of a robotic arm to follow a path on a surface. Such a task is difficult for a human to perform without assistance from the robot, due to impoverished perception (e.g. limited depth information, constrained field of view) of the remote scene (typically on a $2D$ screen) at the teleoperator's end. The proposed divisible shared control decomposes the end effector motion space into two complementary subspaces, one for the human and the other for the robot, such that each agent independently controls the motion within the designated motion subspace. In particular, the robot controls end effector orientation and motion normal to the object surface, while the human controls motion tangential to the object surface. We designed and carried out an experiment to investigate user performance and work load with and without the shared control, including the use of a concurrent secondary task to test the cognitive load. Both quantitative measures, such as path error and jerk, and qualitative measures, such as frustration and mental demand, are employed to evaluate the effect.

The authors are with the Institute for Infocomm Research, A*STAR, Singapore 138632.

*Corresponding author (E-mail: kptee@i2r.a-star.edu.sg).

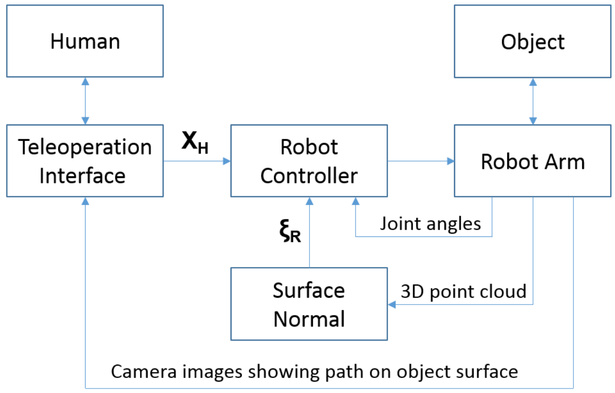

Fig. 1: Divisible shared control scheme for path following task on a smooth surface

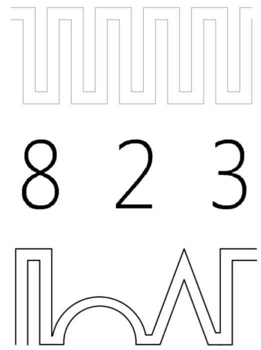

Fig. 2: Task patterns *straight* (top), *numeric* (middle), and *mixed* (bottom) for teleoperated tracing.

II. Divisible Shared Control for Teleoperation Assistance

In this section, we formulate the divisible shared control problem for teleoperated motion control on or near a surface. An example task is that of following a path on an object's surface.

Consider a smooth surface in Euclidean space described by $S(X) = k$, where $X \in \mathbb{R}^3$ are coordinates relative to a world frame, k a constant number, and gradient ∇S is continuous and non-zero at any point on the surface. Then, at any point X_S on the surface, the unit normal is given by:

$$\mathbf{n}(X_S) = \frac{\nabla S(X_S)}{\|\nabla S(X_S)\|} \tag{1}$$

and the tangent plane:

$$\mathbf{t}(X, X_S) = \{X \in \mathbb{R}^3 \mid \mathbf{n}(X_S) \cdot (X - X_S) = 0\} \tag{2}$$

Divisible shared control decomposes the motion space of the end effector into two complementary subspaces, namely $X_H \in \mathbb{R}^3$ and $\xi_R = (X_R, R_R) \in \mathbb{R}^3 \times SO(3)$, such that

$$X_H \cdot X_R = 0 \tag{3}$$
$$X_H \cup \xi_R \in SE(3) \tag{4}$$

The control of end effector motion in X_H is allocated to the human and ξ_R to the robot controller. For a surface path following task, an intuitive division of the motion space is one in which the robot controls the distance of the end effector to the surface, together with the orientation of the end effector with respect to the local surface normal, while the human controls the motion of the end effector on the surface. Such a division makes sense because it is very difficult for the human to accurately perceive errors in the end effector orientation and the distance from the surface, given a $2D$ view of the remote scene, while it is easy for the robot to do so using $3D$ sensors. On the other, the human can easily see the on-surface path errors, so this divisible shared control scheme allows the human to easily control where to move on the object surface, while the robot supports the task by ensuring that the end effector is properly oriented and close to (or touching) the object surface.

The robot's translational control is defined as:

$$X_R = \mathbf{n}(X_s) \tag{5}$$
$$X_s = \underset{X_s \in X_S}{\arg\min} \|X_e - X_s\| \tag{6}$$

where X_e is the end effector position. In other words, the robot controls the translational motion along the normal direction to the object surface at a point X_s on the surface that is closest to the end effector. For locally convex surfaces (e.g. spheres), X_s is unique if it exists within a neighborhood of the end effector.

Besides controlling end effector motion in X_R, the robot also controls its orientation fully, so that it points perpendicularly towards the object surface. Let the end effector frame be $R_e = [\mathbf{r}_x, \mathbf{r}_y, \mathbf{r}_z]$. Then, we can express the desired orientation as

$$R_R = [\mathbf{t}_1, \mathbf{t}_1 \times \mathbf{n}, \mathbf{n}] \tag{7}$$

where $\mathbf{t}_1$ is a unit vector obtained by projecting $\mathbf{r}_x$ onto the tangent plane $\mathbf{t}$:

$$\mathbf{t}_1 = \mathrm{proj}_{\mathbf{t}}(\mathbf{r}_x) = \mathbf{r}_x - \frac{\mathbf{r}_x \cdot \mathbf{n}}{\|\mathbf{n}\|^2}\mathbf{n} \tag{8}$$

The motion subspace controlled by the human lies on the tangent plane at the point X_s on the object surface:

$$X_H \in \mathbf{t}(X_s) \tag{9}$$

As a summary, Figure 1 shows the divisible shared control scheme based on the aforementioned division of end effector motion space into complementary subspaces, for a path following task on a smooth object surface.

III. Teleoperation Experiment

An experiment was designed and performed to investigate the effect of divisible shared control on performance and workload when performing teleoperation tasks involving tracing patterns on a spherical surface with a marker pen mounted at the robot end effector.

Ten subjects (8 male, 2 female) between 17 to 40 years of age participated in the experiment, none of which had prior training with the task, but most had some robotics

Fig. 3: The teleoperation interface displays views of the remote scene and enables the subject to control the robot's motion through a haptic device.

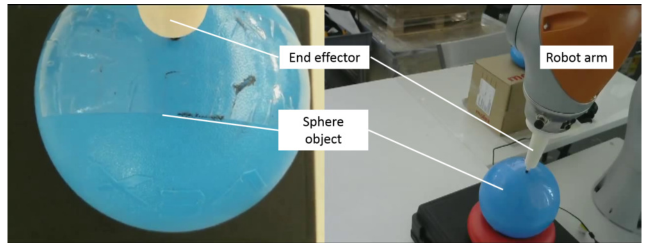

Fig. 4: Views of the sphere object, end effector and robot arm on the teleoperation interface.

background or experience working with robots. One of the subjects was left-handed, and the rest right-handed.

Three task patterns were considered, as shown in Figure 2. Task pattern *straight* consists of alternating lateral and longitudinal straight segments with no disjoints. Task pattern *numeric* consists of mostly curved segments in the form of numeric symbols, with disjoints between the symbols. Task pattern *mixed* consists of a mixture of straight and curved segments with no disjoints. The task patterns were printed on white paper, cut out, and pasted on the top surface of three identical sphere objects of radius $0.1m$, allowing for convenient changeover between experimental conditions.

The teleoperation interface consists of a right-handed `Omega7` haptic device and a 40-inch display, as shown in Figure 3. A subject, seated about $1m$ from the display, holds the haptic device with his/her right hand to control the end effector of a `Kuka iiwa` robot arm. The robot arm is about $1.5m$ to the left of the subject and is out of view when the subject fixates on the display in front of him/her. The display screen shows two views (see Figure 4) to the subject, one from a webcam mounted on the end effector, and one from another webcam mounted on a tripod. The former provides a close-up view of the pen tip moving near or on the object surface, as well as the task pattern, while the latter shows the entire robot arm and the object from a fixed external point of view.

The experiment protocol is as follows. The subject was given both written and verbal instructions on the task to be performed, as well as the four experimental conditions to be tested:

1) `M`: manual mode (i.e. no shared control)
2) `A`: assisted mode (i.e. shared control)
3) `MS`: manual mode with secondary task
4) `AS`: assisted mode with secondary task

The primary task was to trace the pattern on the object, from the start point to the end, using the marker pen mounted on the end effector. The secondary task involved mental addition of two integers audibly presented by computer speakers, and the subject has to give the answer vocally.

After informed consent was obtained, the subject familiarize himself/herself using the haptic device to teleoperate the robot arm, so as to minimize performance gains due to learning effects. Then, the experiment was started, and the subject worked on task pattern *straight* under the conditions `M`, `A`, `MS`, and `AS`, in this order. For each condition, the subject performed the task twice. On completion of the tasks for this task pattern under all four conditions, the subject filled out a questionaire assessing their work load, before repeating the tasks for a different task pattern *numeric*, and finally for task pattern *mixed*.

IV. Evaluation Measures

Both quantitative measures of task performance and qualitative measures of operator workload are used for evaluation of shared control for the teleoperation tasks.

A. Quantitative Measures

We define the following quantitative measures:

1) Total task duration, $T = t_f - t_0$, where t_f is the final time and t_0 the initial time.
2) Integral normed error, given by:
$$E = \int_{t_0}^{t_f} \|e(t)\| dt \tag{10}$$
where $e(t)$ is the shortest vector from the endpoint position $x(t)$ to the task pattern.
3) Integral normed jerk, given by:
$$Jrk = \int_{t_0}^{t_f} \|jrk(t)\| dt \tag{11}$$
where $jrk(t)$ is the filtered jerk obtained by numerically differentiating the filtered endpoint position $x(t)$. We use a tenth-order Butterworth low pass filter with normalized frequency of 0.05.
4) Variance of duration for short and long segments of task pattern *straight*:
$$\nu_{short} = \sigma(s_1, s_2, ..., s_n) \tag{12}$$
$$\nu_{long} = \sigma(l_1, l_2, ..., l_n) \tag{13}$$
where $\sigma(\bullet)$ is the standard deviation of $\bullet$, and s_i, l_i denote the ith short and long segments, respectively.
5) Secondary task score
$$S = \frac{N_c}{N_c + N_w} \frac{T_{\min}}{T} \tag{14}$$
where N_c is the number of correct answers, N_w wrong answers, and $T_{\min}$ the minimum duration over all subjects, with and without shared control, for the

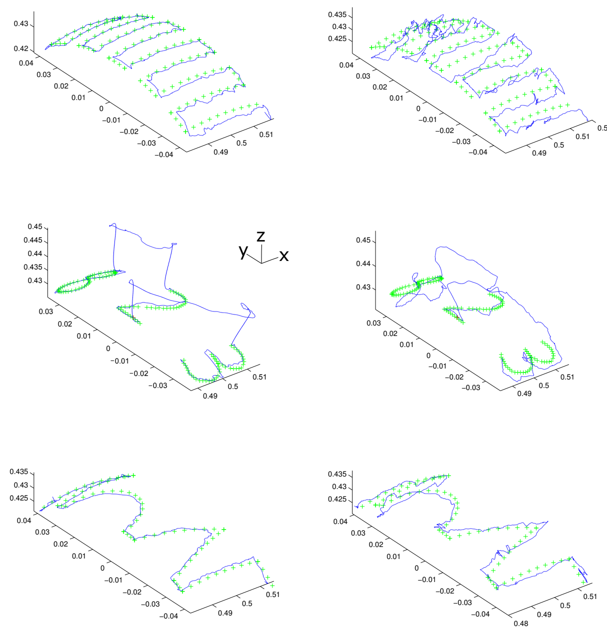

(a) Assisted (b) Manual

Fig. 5: Endpoint paths for task pattern *straight* (top), *numeric* (middle), and *mixed* (bottom), with and without shared control. Green '+' markers indicate points on the desired path.

same task pattern. Note that $T_{\min}$ is for normalization purpose and ensures that the maximum secondary task score is in the interval $[0, 1]$.

B. Qualitative Measures

For qualitative measures of operator workload, we used a subset of questions from the `NASA TLX` questionnaire, which asked subjects to assess themselves on mental demand, physical demand, performance, effort and frustration, each based on a 21-point scale (lower is better). Specifically, subjects were asked the following questions:

1) Mental Demand (1: low – 21: high):
   How mentally demanding was the task?
2) Physical Demand (1: low – 21: high):
   How physically demanding was the task?
3) Performance (1: high – 21: low):
   How successful were you in accomplishing what you were asked to do?
4) Effort (1: low – 21: high):
   How hard did you have to work to accomplish your level of performance?
5) Frustration (1: low – 21: high):
   How insecure, discouraged, irritated, stressed and annoyed were you?

To normalize the scores in a way that is more comparable between subjects, we use the maximum and minimum scores for each subject and re-scale all the scores for that subject

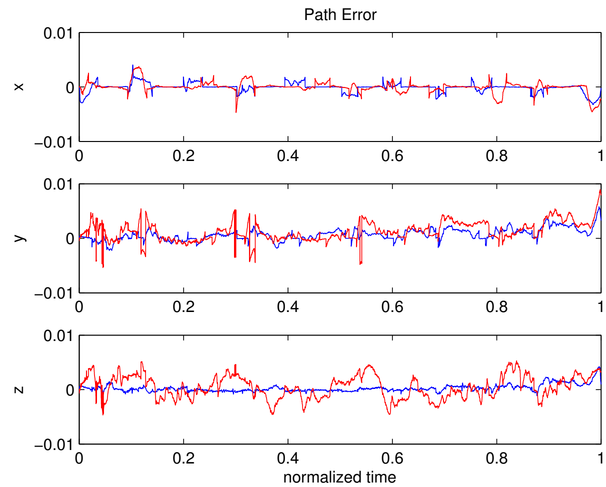

Fig. 6: Single subject's path error for task pattern *straight* with (blue) and without (red) shared control.

to be between 1 and 10. The normalized score Q_{norm} is:

$$Q_{norm} = 1 + \frac{9(Q - Q_{\min})}{Q_{\max} - Q_{\min}} \quad (15)$$

where $Q_{\min}$ and $Q_{\max}$ are the minimum and maximum scores, respectively, for each subject.

V. Results and Evaluation

In this section, we examine both the quantitative and qualitative (subjective) effects of divisible shared control.

A. Quantitative Effects

The effect of shared control on the integral normed error (10) can be clearly seen in Figure 5. Without shared control (i.e. manual mode), the path of the robot end effector as controlled by the user diverges erratically from the desired path on the spherical surface. Many kinks are seen on the paths, indicating jerky motions. However, with shared control (i.e. assisted mode), not only are path errors markedly reduced, but also the motions are smoother. This is true for all three task patterns. Note that for task pattern *numeric*, the path departs from the sphere surface to move from the end of one number pattern to the next, since the number patterns are separated on sphere surface.

Figure 6 shows how the path error in each direction of the sphere's frame changes with time for task pattern *straight*. The error in the z-direction is the largest for the manual mode, as expected, since the user is unable to perceive the z-error well on a $2D$ display screen. With shared control, the z-error is drastically reduced since the robot took over the motion control in the direction of the normal to the sphere's surface. The other two task patterns show similar results.

As shown in the top row of Figure 7, the integral normed error is significantly reduced when shared control is active. This effect is consistent for all three task patterns on the sphere surface, and also in the presence of a secondary task where the user had to perform mental arithmetics while teleoperating the robot. No significance difference was

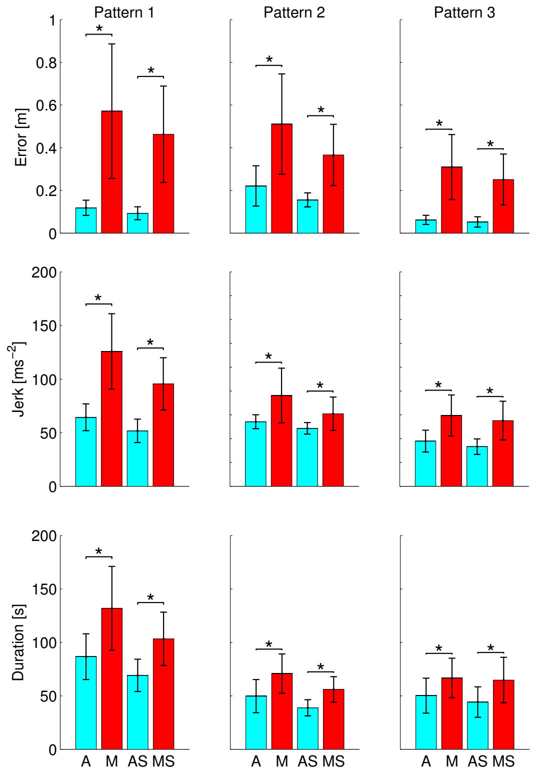

Fig. 7: Quantitative measures of performance, namely error (top), jerk (middle), and duration (bottom). Lower is better. A and M denote with and without shared control respectively. AS and MS denote presence of secondary task for A and M, respectively. Asterisk '*' indicates significant difference ($p < 0.05$).

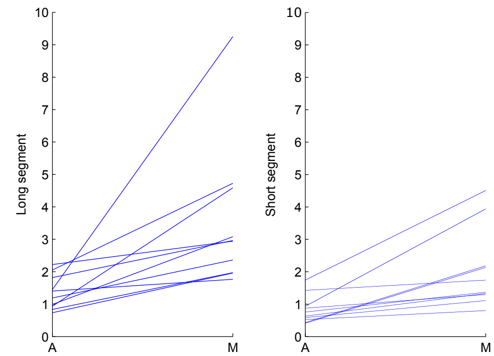

Fig. 8: Standard deviation of duration to complete different segments of task pattern *straight* increases in the absence of shared control. A and M denote with and without shared control respectively. Each line corresponds to a different subject. With shared control, inter-subject variance in the standard deviation values is reduced and similar for both long and short segments.

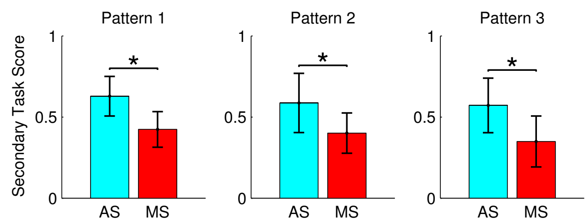

Fig. 9: Secondary task score with (AS) and without (MS) shared control (higher is better). Asterisk '*' indicates significant difference ($p < 0.05$).

observed between A and AS, nor between M and MS. There is a small decrease in mean from A to AS and from M to MS. This could be due to the users becoming familiarized with the task and showing improved performance, since AS and MS trials follow A and M trials respectively.

The integral normed jerk (11) is significantly reduced when there is shared control, as seen in the middle row of Figure 7. This is true for all task patterns, with and without the secondary task. The effect is more pronounced in task patterns *straight* and *mixed*, but less in task pattern *numeric*. This is likely due to the fact that task pattern *numeric* requires additional up-lateral-down motions when advancing from one numeric symbol to the next. Even though shared control helps to smoothen the path-following motions on the sphere's surface, the up-lateral-down motions contribute to the integral normed jerk, resulting in a smaller reduction of the jerk measure than expected.

In terms of task completion time, the bottom row of Figure 7 shows that it similarly decreases with the help of shared control, for all task patterns, with and without the secondary task. The completion for task pattern *straight* is the longest because the total path distance is the greatest, and also involves the most number of sharp turns, which are difficult for most users to follow accurately. From Figure 8, we see that the standard deviation of the completion time increases without shared control, for both long and short segments of task pattern *straight*, for all subjects. Inter-subject variance in the standard deviation values is high without shared control, and long segments of the task pattern produce greater variance than short segments. However, with shared control, inter-subject variance in the standard deviation values is low and similar for both long and short segments. This suggests that shared control can be helpful in reducing the variance of performance, or ensuring the consistency of performance, across users with different skills and proficiency.

Although the secondary task had no effect on the error, jerk, and duration, we observed an effect of shared control on the secondary task performance. The secondary task score increased in the presence of shared control for all task patterns, suggesting that cognitive load is reduced through the role of the robot in assisting the motion control that is difficult for the user, thus giving them more cognitive resources to attend to the secondary task.

B. *Qualitative Effects*

Qualitative effects of shared control were assessed from the normalized score (15) obtained from the NASA TLX questionaire. As evidenced from Figure 10, where it is noted that lower scores are better, subjects rated themselves to have performed better and used less effort when assisted by shared control, for all task patterns. On average, they rated them-

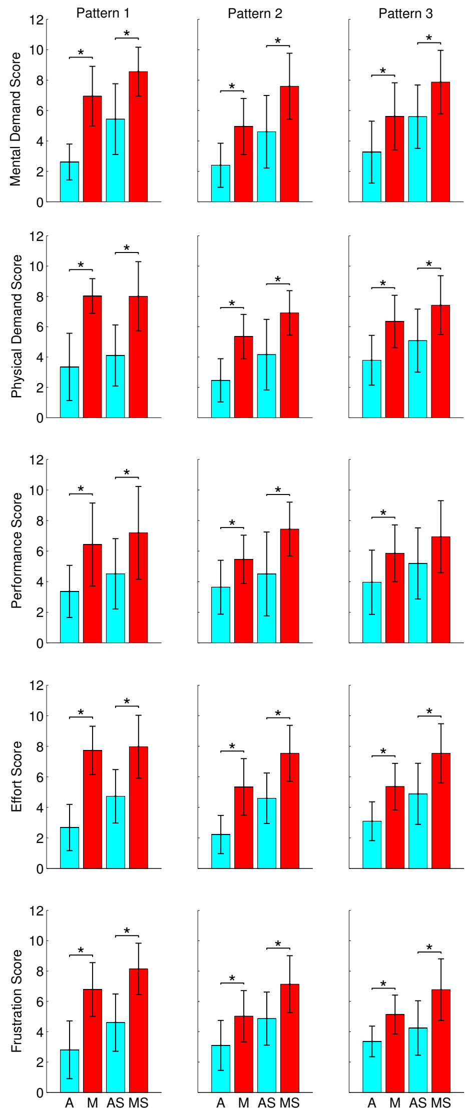

Fig. 10: Qualitative scores from questionnaire (lower is better). Asterisk '*' indicates significant difference ($p < 0.05$).

selves to have performed worse when there was a secondary task, even though actual quantitative performance is slightly better on average (see Figure 7). This perception may be biased by the difficulty and frustration of the performing both primary and secondary tasks simultaneously.

Subjects felt that both mental and physical demands of performing the task increased without assistive shared control from the robot. This is consistent for all task patterns and for the case where there was a secondary task. Similarly, self-rated frustration increased without shared control for all task patterns with and without secondary task. These qualitative results suggest that shared control helped to reduce perceived cognitive and physical load, as well as frustration with a task that is difficult to perform.

VI. Conclusion

This paper has presented an experimental evaluation of a form of divisible shared control suitable for teleoperation tasks on or near an object surface (e.g. painting, blasting). In particular, the robot controls end effector orientation and motion normal to the object surface, while the human controls motion tangential to the object surface. It was shown, based on both quantitative and qualitative measures, that this way of dividing the control between human and robot improves the accuracy, speed, and smoothness of the task motion, and also reduces the cognitive load, effort, and frustration of the human. Interestingly, it was also found that the shared control helped in reducing the variance of performance across different users.

Acknowledgements

We are grateful to Colleen Stevens, Wei Liang Chan, and Yuanwei Chua for fruitful discussions on the experiment design and implementation.

References

[1] S. Hirche and M. Buss, "Human-oriented control for haptic teleoperation," *Proceedings of the IEEE*, vol. 100, pp. 623–647, 2012.

[2] C. Passenberg, A. Peer, and M. Buss, "A survey of environment-, operator-, and task-adapted controllers for teleoperation systems," *Mechatronics*, vol. 20, no. 7, pp. 787 – 801, 2010.

[3] A. Cherubini, R. Passama, A. Crosnier, A. Lasnier, and P. Fraisse, "Collaborative manufacturing with physical humanrobot interaction," *Robotics and Computer-Integrated Manufacturing*, vol. 40, pp. 1 – 13, 2016.

[4] R. Li, Y. Li, S. E. Li, E. Burdet, and B. Cheng, "Driver-automation indirect shared control of highly automated vehicles with intention-aware authority transition," in *2017 IEEE Intelligent Vehicles Symposium (IV)*, 2017, pp. 26–32.

[5] E. Burdet, Y. Li, S. Kager, K.S.G. Chua, A. Hussain, and D. Campolo, "Chapter 10 - interactive robot assistance for upper-limb training," in *Rehabilitation Robotics*, R. Colombo and V. Sanguineti, Eds., pp. 137 – 148. Academic Press, 2018.

[6] N. Jarrasse, T. Charalambous, and E. Burdet, "A framework to describe, analyze and generate interactive motor behaviors," *PLoS ONE*, vol. 7, no. 11, pp. e49945, 2013.

[7] M. S. Erden and B. Maric, "Assisting manual welding with robot," *Robotics and Computer-Integrated Manufacturing*, vol. 27, no. 4, pp. 818–828, 2011.

[8] K. Sreekanth, D.M. Mohan, H. Bo, and D. Campolo, "Manual guidance of a compliant manipulator during curve-following tasks: Basic framework and preliminary experimental tests," in *IEEE Region 10 Conference (TENCON)*, 2016, pp. 3534–3537.

[9] D. Aarno, S. Ekvall, and D. Kragic, "Adaptive virtual fixtures for machine-assisted teleoperation tasks," in *Proceedings of the 2005 IEEE International Conference on Robotics and Automation*, 2005, pp. 897–903.

[10] M. Li, M. Ishii, and R. H. Taylor, "Spatial motion constraints using virtual fixtures generated by anatomy," *IEEE Transactions on Robotics*, vol. 23, no. 1, pp. 4–19, 2007.

[11] J.J. Abbott, P. Marayong, and A.M. Okamura, "Haptic virtual fixtures for robot-assisted manipulation," in *Thrun S., Brooks R., Durrant-Whyte H. (eds) Robotics Research. Springer Tracts in Advanced Robotics*, Berlin, Heidelberg, 2007, vol. 28, pp. 49–64, Springer.

[12] Y. Li, K. P. Tee, W. L. Chan, R. Yan, Y. Chua, and D. K. Limbu, "Continuous role adaptation for human-robot shared control," *IEEE Transactions on Robotics*, vol. 31, no. 3, pp. 672–681, 2015.

[13] Y. Li, K. P. Tee, R. Yan, W. L. Chan, and Y. Wu, "A framework of human-robot coordination based on game theory and policy iteration," *IEEE Transactions on Robotics*, vol. 32, no. 6, pp. 1408–1418, 2016.

[14] J. R. Medina, M. Lawitzky, A. Molin, and S. Hirche, "Dynamic strategy selection for physical robotic assistance in partially known tasks," in *2013 IEEE International Conference on Robotics and Automation*, 2013, pp. 1180–1186.

[15] P. Evrard and A. Kheddar, "Homotopy-based controller for physical human-robot interaction," in *RO-MAN 2009 - The 18th IEEE International Symposium on Robot and Human Interactive Communication*, 2009, pp. 1–6.